Systematic study of the symmetry energy under the local density approximation

Jian Liu,[1,*] Zhongzhou Ren,[1,2,3,†] Chang Xu,[1,‡] and Renli Xu[1]

[1]*Department of Physics, and Key Laboratory of Modern Acoustics, Institute of Acoustics, Nanjing University, Nanjing 210093, China*

[2]*Joint Center of Nuclear Science and Technology, Nanjing University, Nanjing 210093, China*

[3]*Center of Theoretical Nuclear Physics, National Laboratory of Heavy-Ion Accelerator, Lanzhou 730000, China*

(Received 8 May 2013; revised manuscript received 3 July 2013; published 27 August 2013)

The nuclear matter symmetry energy $C_{\rm sym}(\rho)$ and its slope parameter L are studied using local density approximation. With this method, the symmetry energy of nuclear matter can be deduced from matter density distributions of finite nuclei. By systematically analyzing the extracted L for different isotopes, the variation trends of values of extracted L along isotopic chains can be obtained. The study can explain why the neutron rich nuclei in isotopic chains such as ^{208}Pb can be used to extract L under local density approximation. By studying the regularity of extracted L for different isotopic chains, we finally obtain the value of L and its error bar: $L = 66 \pm 7$ MeV. Besides, the density dependence parameter γ is constrained to be 0.69 ± 0.07 for the ansatz of symmetry energy $C_{\rm sym}(\rho) = C_{\rm sym}(\rho_0)(\frac{\rho}{\rho_0})^{\gamma}$.

DOI: 10.1103/PhysRevC.88.024324 PACS number(s): 21.65.Ef, 21.10.Gv, 21.65.Mn

I. INTRODUCTION

The symmetry energy $C_{\rm sym}(\rho)$, which represents the energy cost per nucleon to convert all the protons to neutrons in symmetric nuclear matter at the density, ρ, is a currently active field in nuclear physics and astrophysics [1]. Though the equation of state (EOS) of symmetric nuclear matter with equal fractions of neutrons and protons can be relatively well determined over a wide range of densities, our knowledge about asymmetric nuclear matter is very limited because the symmetry energy is undetermined [2,3]. A precise knowledge of EOS of asymmetric nuclear matter is very important for understanding the heavy-ion reactions [3–5], the radioactive nuclei properties [6,7], and many interesting issues in astrophysics [8–12].

The value of slope parameter L of the symmetry energy $C_{\rm sym}(\rho)$ at saturation density ρ_0 is a key point to determine the EOS of asymmetric nuclear matter. In recent years, great efforts have been devoted to determine the value of slope parameter L of the symmetry energy $C_{\rm sym}(\rho)$ at saturation density, however, it is still fraught with many uncertainties. From heavy ion collisions (HIC) method, L is constrained in the range of 50–80 MeV by using the flow of Sn isotopes [13–17]. The refinement of the droplet model (the finite-range droplet model) fixes L to be 70 ± 15 MeV [7]. Fitting the available data on the isobaric analog states predicts $L =$ 78–111 MeV [18]. With the method of isospin diffusion, L is estimated to be 88 ± 25 MeV [8,19]. By analyzing the pygmy dipole resonances of ^{68}Ni and ^{132}Sn, the value of L is extracted to be 64.8 ± 15.7 MeV [20–22]. Besides, astrophysical observations of neutron star masses and radii provide other constraints to $43 < L < 52$ MeV [23].

Information on the density dependence of nuclear symmetry energy can also be obtained from the neutron skin thickness of heavy nuclei because there is strong correlation between L and neutron skin thickness [24–27]. Several experiments of neutron radius have been carried out during the last decade with the hadronic probes [28–32]. In order to obtain the neutron skin thickness in a model independent method, the lead radius experiment (PREx) has been carried out in Jefferson Lab which aims to determine the neutron radius by using the parity violating electron scattering. Last year they reported neutron skin of ^{208}Pb $\Delta R_{np} = 0.33^{+0.16}_{-0.18}$ fm [33]. A reanalysis predicts the value to be $\Delta R_{np} = 0.302 \pm 0.175$ fm [34]. The recent high resolution measurement of electric dipole polarizability can also provide constraint on neutron skin thickness and a value of $\Delta R_{np} = 0.168 \pm 0.022$ fm for ^{208}Pb is obtained with this method [35–38].

Recently, a new effective theoretical method for determining the slope parameter L has been proposed [39]. In this method, the authors deduce the symmetry energy of nuclear matter with the new formula, which is based on the local density approximation [39]. By this approximation, the properties of nuclear matter can be calculated with the density distributions of finite nuclei. Many properties of finite nuclei, such as binding energies, charge radii, and charge distributions, can be determined precisely from experiments and also be described well with the nuclear effective interactions theoretically. Then with local density approximation, the properties of finite nuclei can be used to constrain L. It is reasonable to deduce the symmetry energy of nuclear matter with properties of finite nuclei because the initial constraints on the nuclear symmetry energy are few.

In this paper, the symmetry energy of nuclear matter is systematically studied under the local density approximation. The symmetry energy of nuclear matter is deduced by density distributions of different finite nuclei. In Ref. [39], the authors determined the slope parameter L by choosing heavy spherical nucleus ^{208}Pb. In this article, we choose two isotopic chains Sn and Pb to systematically analyze the symmetry energy. The reason for us to choose these two isotopic chains is because both their proton numbers are magic numbers and they lie in the regions of medium mass nuclei and heavy nuclei,

*liujian.nju@gmail.com
†zren@nju.edu.cn
‡cxu@nju.edu.cn

respectively. For each nucleus, we can extract a value of L with local density approximation. By analyzing the extracted values of L with different isotopes, the variation trends of L along isotopic chains can be obtained. The researches show that the very neutron rich isotopes in isotopic chains can be chosen to deduce the value of slope parameter L under the local density approximation, for example ^{208}Pb is used in Ref. [39]. After systematically studying the general regularity of extracted L, we can obtain saturation values of L for different isotopes. During this procedure, all the known even-even nuclei from stable isotopes to neutron rich isotopes in isotopic chains are taken into considerations.

The paper is organized as follows. In Sec. II we discuss the general properties of asymmetry nuclear matter and present the formula of determining symmetry energy under local density approximation. In Sec. III we analyze the numerical results. Finally, a summary is given in Sec. IV.

II. NUCLEAR SYMMETRY ENERGY AND LOCAL DENSITY APPROXIMATION

The EOS of asymmetric nuclear matter, given by its binding energy per nucleon, can be expressed as sum of power series with isospin asymmetry $\delta = (\rho_n - \rho_p)/\rho$:

$$E(\rho, \delta) = E_0(\rho) + C_{\rm sym}(\rho)\delta^2 + O(\delta^4), \tag{1}$$

where ρ_n, ρ_p, and ρ are the neutron, proton, and matter densities, respectively [40,41]. $E_0(\rho)$ is the EOS of symmetric nuclear matter. The term $C_{\rm sym}(\rho)$ is the nuclear symmetry energy and can be expanded in Taylor series around the saturation density ρ_0:

$$C_{\rm sym}(\rho) = C_{\rm sym}(\rho_0) - L\varepsilon + \frac{K_{\rm sym}}{2}\varepsilon^2 + O(\varepsilon^3), \tag{2}$$

where $\varepsilon = (\rho_0 - \rho)/(3\rho_0)$. $L = 3\rho_0 \frac{\partial C_{\rm sym}(\rho)}{\partial \rho}|_{\rho_0}$ and $K_{\rm sym} = 9\rho_0^2 \frac{\partial^2 C_{\rm sym}(\rho)}{\partial \rho^2}|_{\rho_0}$ are the slope parameter and curvature parameter of the nuclear symmetry energy at ρ_0, respectively.

The binding energy of a finite nucleus can be described by the modified Bethe-Weizsacker mass formula [42]:

$$B(N, Z) = a_v A + a_s A^{2/3} + a_{\rm Coul}\frac{Z^2}{A^{1/3}}[1 - Z^{-2/3}] + a_{\rm sym}X_0^2 A + a_{\rm pair}A^{-1/3}\delta_{np} + E_W, \tag{3}$$

where $X_0 = (N - Z)/A$ and the coefficients a_v, a_s, $a_{\rm Coul}$, and $a_{\rm pair}$ are the volume, surface, Coulomb, and pairing energy terms, respectively. The pairing term δ_{np} can be found in Ref. [43]. $a_{\rm sym}$ corresponds to the symmetry energy term. There are several parametrizations for $a_{\rm sym}$ and in this paper we choose the definition

$$a_{\rm sym}(A) = C_v - C_s A^{-1/3}, \tag{4}$$

where C_v and C_s are volume and surface coefficients, respectively. The reason to choose this form of parametrization is that their coefficients have been determined quite precisely by method of the double differences of "experimental" symmetry energies recently in Ref. [44]. The volume coefficient C_v in Eq. (4) corresponds to the symmetry energy $C_{\rm sym}(\rho_0)$ of nuclear matter because the surface contribution vanishes in Eq. (4) if $A \to \infty$. Therefore, Eq. (4) can be rewritten into

$$a_{\rm sym}(A) = C_{\rm sym}(\rho_0) - C_s A^{-1/3}. \tag{5}$$

The coefficients $C_{\rm sym}(\rho_0)$ and C_s have been constrained to be 32.10 ± 0.31 MeV and 58.91 ± 1.08 MeV, respectively, in Ref. [44] with the new method.

As we know that the symmetry energy $C_{\rm sym}(\rho)$ can be represented with the ansatz

$$C_{\rm sym}(\rho) = C_{\rm sym}(\rho_0)\left(\frac{\rho}{\rho_0}\right)^\gamma, \tag{6}$$

where γ reflects the density dependence of the symmetry energy. This form of ansatz is widely used in many theoretical calculations and experimental analysis for heavy-ion collisions [8,14,45,46]. With Eq. (6), we can obtain slope parameter

$$L = 3\rho_0 \frac{\partial C_{\rm sym}(\rho)}{\partial \rho}\bigg|_{\rho_0} = 3\gamma C_{\rm sym}(\rho_0). \tag{7}$$

Also, expanding the symmetry energy into Taylor series around ρ_0 and keeping terms to second order, we can obtain

$$C_{\rm sym}(\rho) \simeq C_{\rm sym}(\rho_0)\left[1 + \gamma\left(\frac{\rho - \rho_0}{\rho_0}\right) + \frac{\gamma(\gamma - 1)}{2!}\left(\frac{\rho - \rho_0}{\rho_0}\right)^2\right]. \tag{8}$$

The symmetry energy term $a_{\rm sym}(A)$ for finite nuclei is always less than $C_{\rm sym}(\rho_0)$ because of the surface contribution in Eq. (5). An equivalent density ρ_A can be defined which makes the $a_{\rm sym}(A)$ equate to $C_{\rm sym}(\rho_A)$ [6,30,31,39,47–49]. With this definition and Eq. (5), we can obtain

$$C_s A^{-1/3} = C_{\rm sym}(\rho_0) - C_{\rm sym}(\rho_A). \tag{9}$$

Then with the relation of Eq. (8), we can deduce

$$C_s = 3\,C_{\rm sym}(\rho_0)A^{1/3}\left[\gamma\varepsilon_A - \tfrac{3}{2}\gamma(\gamma - 1)\varepsilon_A^2\right], \tag{10}$$

where $\varepsilon_A = (\rho_0 - \rho_A)/(3\rho_0)$.

Because the matter distributions of finite nuclei are almost constants at inner region and the densities drop very fast near the surface, therefore, the symmetry energy term $a_{\rm sym}(A)$ for finite nuclei can be rewritten under the local density approximation as [50]

$$a_{\rm sym}(A)\left(\frac{N - Z}{A}\right)^2 = C_{\rm sym}(\rho_0)\left(\frac{\rho_A}{\rho_0}\right)^\gamma\left(\frac{N - Z}{A}\right)^2 = \frac{1}{A}\int d^3r\rho(r)C_{\rm sym}(\rho_0)\left(\frac{\rho(r)}{\rho_0}\right)^\gamma \times\left[\frac{\rho_n(r) - \rho_p(r)}{\rho(r)}\right]^2. \tag{11}$$

This is an important relation because by this equation, we can associate the symmetry energy terms $a_{\rm sym}(A)$ of finite nuclei with the density distributions of finite nuclei, which can be described by mean-field models.

The symmetry energy coefficient γ is connected with nuclear density distributions by Eq. (11), if the equivalent density ρ_A is known. Combining Eqs. (10) and (11), the

numerical solutions of γ and corresponding ρ_A can be obtained. For a certain value of γ, we can calculate the corresponding ρ_A with Eq. (11). Then we substitute these two values into Eq. (10) and check whether or not the equation is satisfied. By this way the solutions of γ and ρ_A are obtained. During this procedure, the nuclear matter distributions are obtained from nuclear effective interactions. $C_{\rm sym}(\rho_0)$ and C_s are taken as 32.10 ± 0.31 MeV and 58.91 ± 1.08 MeV, respectively [44], as stated below Eq. (5). The saturation density is taken as 0.155 ± 0.008 fm^{-3} [39], where the error is chosen to encompass the saturation densities calculated from different parameter sets.

III. NUMERICAL RESULTS AND DISCUSSION

In this section, the nuclear symmetry energy $C_{\rm sym}(\rho)$ and slope parameter L are systematically studied with the formula presented in Sec. II. The proton densities and nuclear binding energies can be well reproduced by mean-field models, however, there are uncertainties in neutron density distributions. The nonrelativistic models and relativistic models always give different values of neutron skins of heavy nuclei. Therefore, in this section, both nonrelativistic and relativistic models are used to investigate the symmetry energies. In Ref. [39], the authors have calculated the slope parameter L with the local density approximation and obtained a value $L = 64 \pm 5$ MeV. During their studies, the proton and neutron densities of ^{208}Pb are chosen. However, if a different nucleus is chosen, such as ^{198}Pb, the final result for L also changes correspondingly. Therefore, in this section, based on the studies of Ref. [39], we extract the values of L with local density approximation where the corresponding nuclei are chosen to be both the medium mass Sn isotopes and heavy Pb isotopes. Then the variation trends of L with the isospin asymmetry $X_0 = (N - Z)/A$ is analyzed.

First, the values of L extracted from the medium mass Sn isotopes under local density approximation are investigated. All the even-even nuclei with mass number ranging from 108 to 134 are chosen. The results cover the stable isotopes and very neutron rich isotopes that are experimentally known. Different parameter sets are used to generate the density distributions of Sn isotopes, such as the nonrelativistic sets: SIII, SkP, SkM*, SLy4, SLy5, as well as the relativistic sets: NL-SH, NL1, NL2, NL3, NL3*, TM1, FSU, and IU-FSU.

In Fig. 1, we present the variations of values of L with the isospin asymmetry $X_0 = (N - Z)/A$ where the corresponding matter densities of Sn isotopes are calculated from FSU and NL3 parameter sets, respectively. From this figure we can see that the extracted L first decreases rapidly with the increasing of isospin asymmetry $X_0 = (N - Z)/A$. However, when the isospin asymmetry X_0 becomes larger than 0.17 (corresponding to ^{120}Sn), the extracted L is almost unchanged and a saturation value of L is reached. By calculating the average of extracted L from last four even-even isotopes, we finally obtain the saturation value $L = 68.8$ MeV and $L = 64.7$ MeV for the FSU and NL3 parameter sets, respectively.

The reason for changes of L along the isotopic chain in Fig. 1 is due to the local density approximation in Eq. (11). Equation (11) is mathematically strict if the nuclear matter

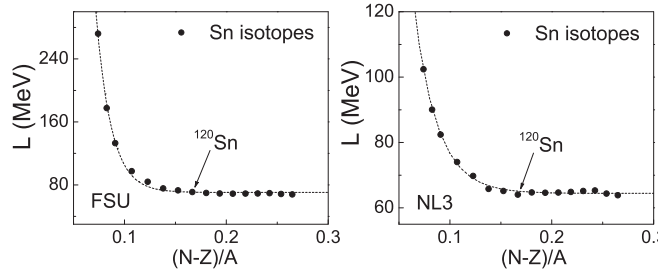

FIG. 1. Variations of values of L along the Sn isotopic chain. The nuclear matter distributions of Sn isotopes in Eq. (11) are calculated from relativistic FSU and NL3 parameter sets, respectively. The dash lines in the figures are used to show the changing trends.

density distributions are sharp-surface density distribution $\rho(r) = \rho_0\Theta(R_0 - |r|)$ where $\Theta(R_0 - |r|)$ is a step function. However, for theoretical matter density distributions obtained from mean-field models, there are fluctuations at the inner region and diffuseness at the surface. Therefore, Eq. (11) is valid approximately for real nuclear matter distributions. In Fig. 2, we present the distributions of the local density asymmetry $X(r) = \frac{\rho_n(r)-\rho_p(r)}{\rho(r)}$ and $\rho(r)[X(r)]^2$ for some Sn isotopes. From the left panel of Fig. 2, we can observe that with the increasing of isospin asymmetry X_0, distributions of $X(r)$ gradually get close to the sharp-surface distributions. This causes $\rho(r)[X(r)]^2$ dropping much faster at the nuclear surface for the neutron rich Sn isotopes. In the range of nuclear size, the term $C_{\rm sym}(\rho_0)(\frac{\rho(r)}{\rho_0})^\gamma$ in Eq. (11) is almost a constant. Therefore, if distributions of $\rho(r)[X(r)]^2$ drop faster at the surface, the approximation Eq. (11) works better. This results in a very small change of extracted L for the neutron rich Sn isotopes, which can be observed in Fig. 1.

Besides the medium mass Sn isotopes, the heavy Pb isotopes are also chosen to study the symmetry energy of nuclear matter. All the even-even isotopes with mass number ranging from 182 to 220 are taken into considerations. The slope parameter L are systematically calculated by Eqs. (10) and (11) where the corresponding matter density distributions of Pb isotopes are calculated with different parameter sets. The results of FSU and NL3 parameter sets are presented in Fig. 3. In this figure we can also see firstly the extracted L decreases rapidly with the increasing of isospin asymmetry. When the isospin asymmetry X_0 is larger than 0.21 (corresponding to ^{208}Pb), the changes of extracted L are very small. Compared

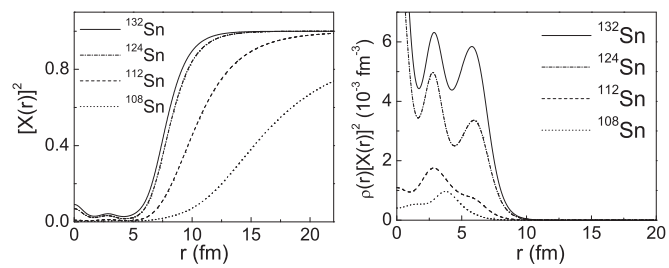

FIG. 2. Distributions of the local density asymmetry $X(r) = \frac{\rho_n(r)-\rho_p(r)}{\rho(r)}$ and $\rho(r)[X(r)]^2$ for ^{108}Sn, ^{112}Sn, ^{124}Sn, and ^{132}Sn, which are calculated from FSU parameter set.

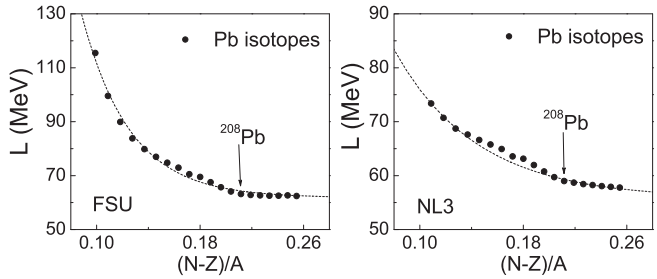

FIG. 3. Variations of values of L along the Pb isotopic chain. The nuclear matter distributions of Pb isotopes in Eq. (11) are calculated from relativistic FSU and NL3 parameter sets, respectively. The dashed lines are used to show the changing trends.

with Sn isotopes in Fig. 1, the data do not saturate very well for the heavy Pb isotopes but the changes of extracted L are less than 2 MeV for the last our even-even isotopes. Therefore, we also use the averages of extracted L from last four even-even isotopes to represent their saturation values. Finally we obtain the saturation value $L = 62.6$ MeV and $L = 57.9$ MeV for FSU and NL3 parameter sets, respectively.

The reason for changes of L along the Pb isotopic chain in Fig. 3 is also due to the local density approximation in Eq. (11). In Fig. 4, we present the distributions of the local density asymmetry $X(r) = \frac{\rho_n(r)-\rho_p(r)}{\rho(r)}$ and $\rho(r)[X(r)]^2$ for some Pb isotopes. It can be seen in this figure that the behavior of $X(r)$ and $\rho(r)[X(r)]^2$ of Pb isotopes is very similar to that of Sn isotopes. The approximation Eq. (11) is more accurate for neutron rich Pb isotopes because their distributions of $\rho(r)[X(r)]^2$ are much closer to the sharp-surface density distributions. Therefore the changes of extracted L are very small if isospin asymmetry X_0 is larger than a certain value for the Pb isotopes, which can be observed in Fig. 3. In the ideal case, L should be a constant along isotopic chains because $L = 3\gamma(a_{\rm sym}(A) + C_s A^{-1/3}) = 3\gamma C_{\rm sym}(\rho_0)$. The changes of extracted L along the Sn and Pb isotopic chains in Figs. 1 and 3 are close to the ideal case, when isospin asymmetry X_0 is larger than a certain value.

Besides FSU and NL3 parameter sets, the saturation values of L for other parameter sets are also studied and the results are presented in Fig. 5 with red squares versus the neutron skin thickness. For purposes of comparison and analysis, we extend the model in Fig. 5 but follow the figure styles of Fig. 1 in Ref. [39]. The shadow represents errors which are generated

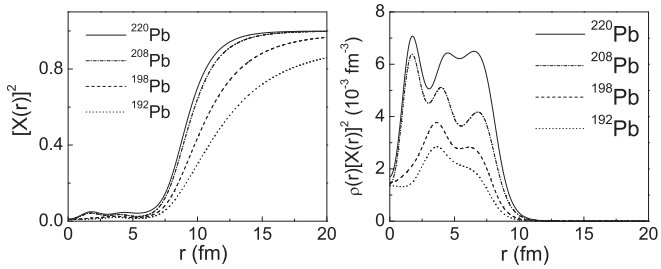

FIG. 4. Distributions of the local density asymmetry $X(r) = \frac{\rho_n(r)-\rho_p(r)}{\rho(r)}$ and $\rho(r)[X(r)]^2$ for ^{192}Pb, ^{198}Pb, ^{208}Pb, and ^{220}Pb, which are calculated from FSU parameter set.

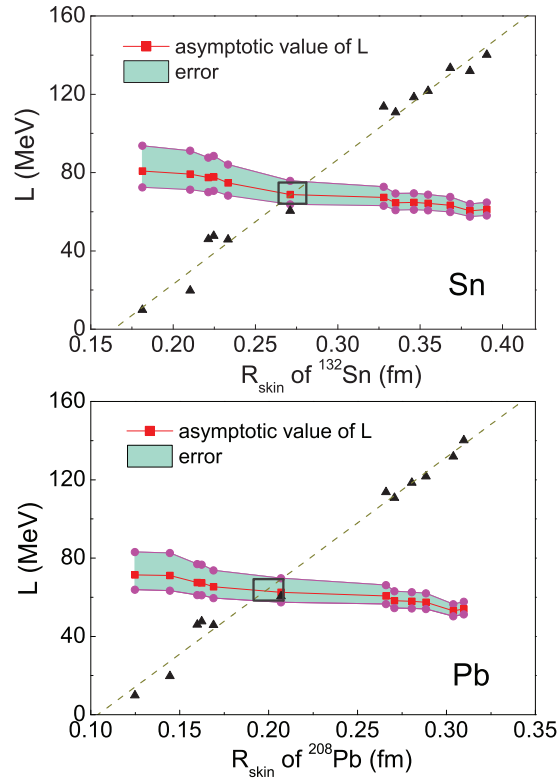

FIG. 5. (Color online) Saturation values of L for different parameter sets versus neutron skins. The neutron and proton density distributions of Sn and Pb isotopes are used in Eq. (11) to deduce these values, respectively. The shadow represents errors which are generated from the uncertainties of $C_{\rm sym}(\rho_0)$, C_s and ρ_0. Triangles represent L calculated from Eqs. (7) and (12) with different interactions. The acceptable window for the values of L is represented by gray rectangle.

from the uncertainties of $C_{\rm sym}(\rho_0)$, C_s, and ρ_0 in Eqs. (10) and (11). For comparison, we also calculate L with Eq. (7) where $C_{\rm sym}(\rho)$ are obtained directly from the calculations of infinite nuclear matter with mean-field models:

$$C_{\rm sym}(\rho) = \frac{k_F^2}{6E_F^*} + \frac{g_\rho^2}{12\pi^2}\frac{k_F^3}{m_\rho^{*2}}. \qquad (12)$$

L calculated from Eqs. (7) and (12) are presented in Fig. 5 with triangles. It can be seen in Fig. 5 that L calculated from different parameter sets with Eqs. (7) and (12) differ considerably, where the nonrelativistic nuclear interactions predict $20 < L < 60$ MeV and most relativistic nuclear interactions lead to $L > 100$ MeV. However, with the local density distribution, the properties of finite nuclei can be used to constrain the slope parameter L. L derived from Eqs. (10) and (11) with different parameter sets are close to each other. The gray box projects out the region of L and $R_{\rm skin}$ that satisfies these two models [Eqs. (10), (11) and Eqs. (7), (12)] simultaneously. From Fig. 5 we finally obtain the value 69 ± 5 MeV for Sn isotopes and 64 ± 5 MeV for Pb isotopes.

The values of L extracted from Pb and Sn isotopes are very close to each other, though their proton numbers differ widely. The deviation of L mainly causes by the surface symmetry energy coefficients C_s in Eq. (10). For medium mass Sn

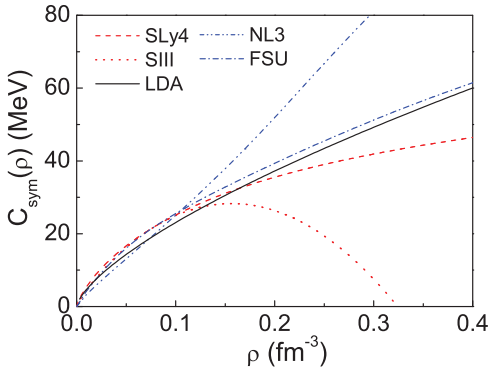

FIG. 6. (Color online) Density dependence of the nuclear symmetry energy $C_{\rm sym}(\rho)$ for different parameter sets. The LDA represents $C_{\rm sym}(\rho)$ which is deduced under local density approximation with Eqs. (10) and (11) in this paper.

isotopes and heavy Pb isotopes, the contributions of surface terms to the symmetry energies in Eq. (5) are different and the value $C_s = 58.91 \pm 1.08$ MeV is an average value which is obtained by fitting binding energies of all nuclei. Besides L obtained from lower panel of Fig. 5 is equal to the result of Ref. [39] where the matter density distributions of ^{208}Pb are used. This is understandable because L deduced from ^{208}Pb is very close to the saturation value of Pb isotopic chain, which can be seen in Fig. 3.

With the results of both Sn and Pb isotopes, we finally obtain an average value $L = 66 \pm 7$ MeV. Besides, with Eq. (7), we can also obtain $\gamma = 0.69 \pm 0.07$ and this value agrees with the result $\gamma \simeq 0.69$ which is obtained from nuclear reaction interpreted by the dynamical and the statistical models of multifragmentation [45]. Submitted γ into Eq. (6), the density dependence of symmetry energy $C_{\rm sym}(\rho)$ can be estimated. Symmetry energy $C_{\rm sym}(\rho)$ deduced under local density approximation is presented in Fig. 6. For comparison, the $C_{\rm sym}(\rho)$ calculated from other parameter sets with Eq. (12) are also presented in this figure. We can see that a stiff form of symmetry energy $C_{\rm sym}(\rho)$ is obtained under the local density approximation.

IV. SUMMARY

In this paper, we investigate the symmetry energy $C_{\rm sym}(\rho)$ and its slope parameter L at the saturation density ρ_0 under the local density approximation. Based on this approximation, the symmetry energy $C_{\rm sym}(\rho)$ of nuclear matter can be deduced from the density distributions of finite nuclei. It is reasonable to deduce the symmetry energy of nuclear matter with properties of finite nuclei because the initial constraints on the nuclear matter are few. Under the local density approximation, the values of L deduced with different parameter sets are very close to each other and can be constrained in a small range.

The proton and neutron densities of Sn and Pb isotopes are chosen to deduce L in this paper. By systematically studying with different isotopic chains, the variation of extracted L along isotopic chains can be analyzed. From analysis of local density asymmetry $X(r)$ and $\rho(r)[X(r)]^2$ for different isotopes, we conclude that the variation of L is due to the local density approximation used in analysis. For different isotopic chains, the saturation values of extracted L are reached for neutron rich isotopes. The researches in this paper demonstrate that the slop parameter L can be extracted from the very neutron rich isotopes in the isotopic chains under local density approximation, for example ^{208}Pb in the Pb isotopic chain. Taking into considerations of the saturation values of L of different isotopic chains, we finally obtain the values $L = 66 \pm 7$ MeV and $\gamma = 0.69 \pm 0.07$ for the ansatz of symmetry energy $C_{\rm sym}(\rho) = C_{\rm sym}(\rho_0)(\frac{\rho}{\rho_0})^\gamma$.

ACKNOWLEDGMENTS

This work is supported by the National Natural Science Foundation of China (Grants No. 11035001, 10735010, 10975072, 11175085, and 11235001), by the 973 National Major State Basic Research and Development of China (Grants No. 2013CB834400 and 2010CB327803), by Research Fund of Doctoral Point (RFDP), Grants No. 20100091110028, by the Project Funded by the Priority Academic Programme Development of JiangSu Higher Education Institutions (PAPD), and by the Research and Innovation Project for College Postgraduate of JiangSu Province, Grant No. CXZZ13_0032.

[1] M. B. Tsang *et al.*, Phys. Rev. C **86**, 015803 (2012).
[2] Chang Xu and Bao-An Li, Phys. Rev. C **81**, 064612 (2010).
[3] P. Danielewicz, R. Lacey, and W. G. Lynch, Science **298**, 1592 (2002).
[4] B. A. Li, Nucl. Phys. A **708**, 365 (2002).
[5] V. Baran, M. Colonna, V. Greco, and M. Di Toro, Phys. Rep. **410**, 335 (2005).
[6] B. A. Brown, Phys. Rev. Lett. **85**, 5296 (2000).
[7] P. Möller, W. D. Myers, H. Sagawa, and S. Yoshida, Phys. Rev. Lett. **108**, 052501 (2012).
[8] B. A. Li, L. W. Chen, and C. M. Ko, Phys. Rep. **464**, 113 (2008).
[9] K. Sumiyoshi and H. Toki, Astrophys. J. **422**, 700 (1994).
[10] J. M. Lattimer and M. Prakash, Science **304**, 536 (2004).
[11] A. W. Steiner, M. Prakash, J. M. Lattimer, and P. J. Ellis, Phys. Rep. **411**, 325 (2005).
[12] C. J. Horowitz and J. Piekarewicz, Phys. Rev. Lett. **86**, 5647 (2001).
[13] M. B. Tsang *et al.*, Phys. Rev. Lett. **92**, 062701 (2004).
[14] M. Famiano *et al.*, Phys. Rev. Lett. **97**, 052701 (2006).
[15] T. X. Liu *et al.*, Phys. Rev. C **76**, 034603 (2007).
[16] M. B. Tsang, Yingxun Zhang, P. Danielewicz, M. Famiano, Zhuxia Li, W. G. Lynch, and A. W. Steiner, Phys. Rev. Lett. **102**, 122701 (2009).
[17] Z. Y. Sun *et al.*, Phys. Rev. C **82**, 051603(R) (2010).
[18] P. Danielewicz and J. Lee, Nucl. Phys. A **818**, 36 (2009).
[19] L. W. Chen, C. M. Ko, and B. A. Li, Phys. Rev. Lett. **94**, 032701 (2005).
[20] A. Klimkiewicz *et al.*, Phys. Rev. C **76**, 051603(R) (2007).
[21] O. Wieland *et al.*, Phys. Rev. Lett. **102**, 092502 (2009).
[22] A. Carbone, Gianluca Colò, Angela Bracco, Li-Gang Cao, Pier Francesco Bortignon, Franco Camera, and Oliver Wieland, Phys. Rev. C **81**, 041301(R) (2010).

[23] A. W. Steiner and S. Gandolfi, Phys. Rev. Lett. **108**, 081102 (2012).
[24] B. G. Todd-Rutel and J. Piekarewicz, Phys. Rev. Lett. **95**, 122501 (2005).
[25] X. Roca-Maza, M. Centelles, X. Viñas, and M. Warda, Phys. Rev. Lett. **106**, 252501 (2011).
[26] Shufang Ban, C. J. Horowitz, and R. Michaels, J. Phys. G: Nucl. Part. Phys. **39**, 015104 (2012).
[27] Jian Liu, Zhongzhou Ren, and Tiekuang Dong, Nucl. Phys. A **900**, 1 (2013).
[28] A. Trzcińska, J. Jastrzębski, P. Lubiński, F. J. Hartmann, R. Schmidt, T. von Egidy, and B. Kłos, Phys. Rev. Lett. **87**, 082501 (2001).
[29] B. Kłos *et al*., Phys. Rev. C **76**, 014311 (2007).
[30] M. Centelles, X. Roca-Maza, X. Viñas, and M. Warda, Phys. Rev. Lett. **102**, 122502 (2009).
[31] M. Warda, X. Viñas, X. Roca-Maza, and M. Centelles, Phys. Rev. C **80**, 024316 (2009).
[32] J. Zenihiro *et al*., Phys. Rev. C **82**, 044611 (2010).
[33] A. Abrahamyan *et al*., Phys. Rev. Lett. **108**, 112502 (2012).
[34] C. J. Horowitz *et al*., Phys. Rev. C **85**, 032501(R) (2012).
[35] P. G. Reinhard and W. Nazarewicz, Phys. Rev. C **81**, 051303(R) (2010).
[36] J. Piekarewicz, Phys. Rev. C **83**, 034319 (2011).
[37] A. Tamii *et al*., Phys. Rev. Lett. **107**, 062502 (2011).
[38] J. Piekarewicz *et al*., Phys. Rev. C **85**, 041302(R) (2012).
[39] B. K. Agrawal, J. N. De, and S. K. Samaddar, Phys. Rev. Lett. **109**, 262501 (2012)
[40] Y. Zhang *et al*., Phys. Rev. C **85**, 024602 (2012).
[41] Chang Xu, Bao-An Li, and Lie-Wen Chen, Phys. Rev. C **82**, 054607 (2010).
[42] N. Wang, Z. Y. Liang, M. Liu, and X. Z. Wu, Phys. Rev. C **82**, 044304 (2010).
[43] Jorge G. Hirsch and Joel Mendoza-Temis, J. Phys. G: Nucl. Part. Phys. **37**, 064029 (2010).
[44] H. Jiang, G. J. Fu, Y. M. Zhao, and A. Arima, Phys. Rev. C **85**, 024301 (2012).
[45] D. V. Shetty, S. J. Yennello, and G. A. Souliotis, Phys. Rev. C **76**, 024606 (2007).
[46] L. W. Chen, C. M. Ko, and B. A. Li, Phys. Rev. C **72**, 064309 (2005).
[47] S. Typel and B. A. Brown, Phys. Rev. C **64**, 027302 (2001).
[48] M. Centelles, M. Del Estal, X. Viñas, and S. K. Patra, in *The Nuclear Many-Body Problem*, Vol. 53 of NATO Advanced Studies Institute Series B: Physics, edited by W. Nazarewicz and D. Vretenar (Kluwer, Dordrecht, 2002), p. 97.
[49] M. Baldo, C. Maieron, P. Schuck, and X. Viñas, Nucl. Phys. A **736**, 241 (2004).
[50] S. K. Samaddar, J. N. De, X. Viñas, and M. Centelles, Phys. Rev. C **76**, 041602(R) (2007).